Eur. Phys. J. A **30**, 391–396 (2006)
DOI 10.1140/epja/i2006-10139-0

THE EUROPEAN PHYSICAL JOURNAL A

Excited states in neutron-rich ^{188}W produced by an ^{18}O-induced 2-neutron transfer reaction

T. Shizuma[1,a], T. Ishii[2], H. Makii[2], T. Hayakawa[1], S. Shigematsu[2,3], M. Matsuda[4], E. Ideguchi[5], Y. Zheng[5], M. Liu[5], T. Morikawa[6], P.M. Walker[7], and M. Oi[7]

[1] Quantum Beam Science Directorate, Japan Atomic Energy Agency, Kizu, Kyoto 619-0215, Japan
[2] Advanced Science Research Center, Japan Atomic Energy Agency, Tokai, Ibaraki 319-1195, Japan
[3] Department of Energy Sciences, Tokyo Institute of Technology, Yokohama 226-8502, Japan
[4] Department of Research Reactor and Tandem Accelerator, Japan Atomic Energy Agency, Tokai, Ibaraki 319-1195, Japan
[5] Center for Nuclear Study, University of Tokyo, Wako, Saitama 351-0198, Japan
[6] Department of Physics, Kyushu University, Fukuoka 812-8581, Japan
[7] Department of Physics, University of Surrey, Guildford, GU2 7XH, UK

Received: 1 September 2006 / Revised: 10 October 2006 /
Published online: 24 November 2006 –
Communicated by J. Äystö

Abstract. Excited states in neutron-rich ^{188}W have been populated using a ^{186}W(^{18}O, ^{16}O) reaction. In-beam γ-rays were measured in coincidence with scattered particles detected by a high-resolution ΔE-E Si telescope. In this experiment, the ground-state band has been identified up to $I^\pi = 8^+$. The γ band, the $K^\pi = 2^-$ octupole band, and a 2-quasiparticle state were also observed. The results are compared with predictions of self-consistent HFB cranking calculations and blocked-BCS multi-quasiparticle calculations.

PACS. 23.20.Lv γ transitions and level energies – 25.70.Hi Transfer reactions – 27.70.+q $150 \leq A \leq 189$

1 Introduction

Neutron-rich W-Os nuclei with $A \approx 190$ exhibit signatures of γ-softness, triaxiality, and a prolate-oblate shape transition [1–4]. In addition, the emergence of high-K isomers (where K is the angular-momentum projection on the symmetry axis) based on multi-quasiparticle configurations is a characteristic of nuclei in this region [5]. The multi-quasiparticle calculations recently performed suggest long-lived isomers existing in neutron-rich ^{188}W [6]. However, little information on the near-yrast structure of ^{188}W has been available because of experimental difficulties. So far, several excited states in neutron-rich ^{188}W, including the $I^\pi = (2^+)$ and (4^+) levels in the ground-state band (GSB), were observed in a (t, p) reaction [7] in which no γ-rays were detected. Recently, three transitions in the GSB were identified, confirming the previous observation [8].

Recent progress in γ-ray spectroscopic techniques using relativistic fragmentation reactions [2] and deep inelastic reactions [3,8,9] has enabled us to investigate the structure of neutron-rich nuclei in the $A \approx 190$ region. In the present work, we employed an ^{18}O-induced 2-neutron transfer reaction to populate excited states in neutron-rich ^{188}W, in conjunction with the in-beam γ-ray spectroscopic method. This type of experimental technique has been applied to neutron-rich trans-uranium nuclei and proven to be effective for the investigation of the near-yrast structure [10,11]. In the heavy-ion transfer reaction, many reaction channels with small cross-sections contribute to the total reaction cross-section. A high-resolution particle detector is therefore necessary for clear identification of the products.

2 Experiments

The present experiment was performed at the tandem accelerator facility, JAEA, Tokai [12]. Excited states of ^{188}W were populated using the ^{186}W(^{18}O, ^{16}O) reaction. The 180 MeV ^{18}O beam with the average current of 0.3 particle nA was incident on a self-supporting target of ^{186}W enriched to 98.2%. The cross-section of the reaction employed was estimated to be ~ 0.1 mb. The irradiation time was approximately 80 hours. The target was made of two stacked 450 μg/cm^2 metallic foils and thick enough to stop target-like nuclei inside the target material. Outgoing projectile-like ions were detected by four sets of surface barrier Si ΔE-E detectors with a diameter of 20 mm. These detectors were placed at 28° with

[a] e-mail: shizuma.toshiyuki@jaea.go.jp

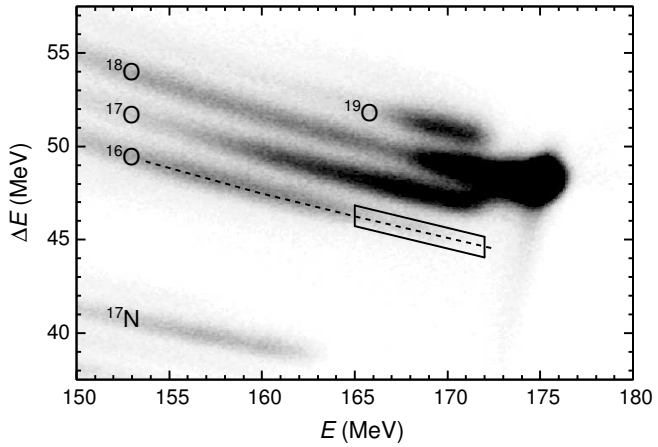

Fig. 1. E-ΔE plot for ions measured by the Si detectors. The dashed line shows calculated energy losses for ^{16}O. The enclosed area drawn with a solid line represents the gate window used for the present analysis.

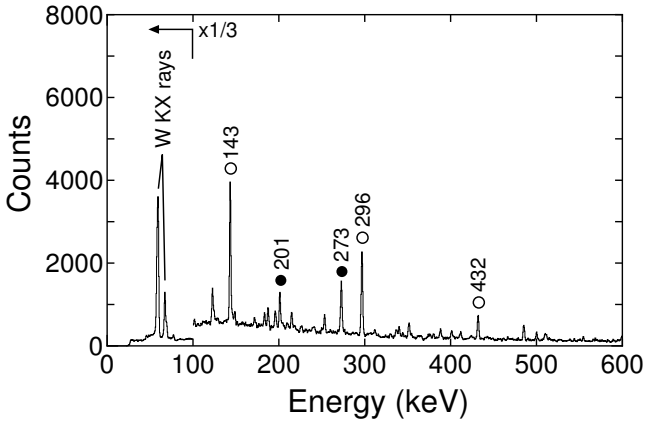

Fig. 2. A γ-ray energy spectrum gated on ^{16}O particles with kinetic energies between 165 and 172 MeV (see the enclosed area in fig. 1). The γ-ray transitions in ^{188}W and ^{187}W are marked by open and filled circles, respectively.

respect to the beam direction, at a distance of 5 cm from the target position. The thickness of the Si ΔE detectors, ground by the electrolytic in-process dressing method, was $83 \pm 1\,\mu$m. A ring-shaped aluminium plate was placed in front of the Si detectors so that ions scattered at angles less than 21° could not hit the Si detectors. A solid angle of 0.4 sr is therefore covered with scattering angles between 21° and 35°.

Photons emitted from the residual nuclei were measured by seven HP-Ge detectors, in coincidence with the outgoing ions. Four of these detectors, with relative efficiency of 60%, were arranged symmetrically in a plane perpendicular to the beam axis at a distance of 6 cm from the target position. Two of the four Ge detectors and two of the Si ΔE-E detectors were placed in the horizontal plane including the beam axis, while the other two Ge detectors and two Si ΔE-E detectors were in the vertical plane. This setup allows us to extract γ-ray anisotropies and to deduce transition multipole orders. The remaining three Ge detectors with relative efficiency of 30–40% were installed between the four Ge detectors stated above.

The time difference (Δt) between signals from the Si and Ge detectors was measured by time-to-amplitude converters (TAC). The TAC range was set to 2 μs. Energy and time information on outgoing ions and γ-rays was recorded event by event on magnetic tapes. A total of 1.6×10^8 and 6.8×10^7 events for particle-γ and particle-γ-γ coincidences, respectively, were collected. Energy and efficiency calibration of the Ge detectors was made using standard γ-ray sources of ^{133}Ba, ^{152}Eu, and ^{241}Am.

3 Results

An E-ΔE plot for outgoing ions measured by the Si detectors is shown in fig. 1. The ions are clearly separated by mass number as well as atomic number. The particle energies were calibrated assuming that the most intense peak in the E-ΔE plot corresponds to elastically scattered events of ^{18}O ions entering at the center of the each Si detector. The dashed line in fig. 1 represents calculated energy losses for ^{16}O, and reproduces well the measured values. Figure 2 shows a γ-ray energy spectrum gated on ^{16}O particles with kinetic energies between 165 and 172 MeV (the enclosed area drawn in fig. 1). The γ-ray transitions in the GSB of ^{188}W can be seen. In fig. 2, γ-ray peaks from ^{187}W are also observed. This nucleus can be produced by one-neutron evaporation from ^{188}W following the 2-neutron transfer, when the compound-like ^{188}W is excited above the neutron separation energy of 6.8 MeV. The higher-energy ^{16}O gate therefore gives clean γ-ray spectra for ^{188}W.

Since the angular momentum of the residual nuclei produced in heavy-ion transfer reactions is polarized perpendicular to the reaction plane defined by the directions of incoming and outgoing ions, the angular distribution of γ-rays emitted from such nuclei is anisotropic. In the present work, this anisotropy is given as an intensity ratio of γ-rays detected by the Ge detectors placed *in* and *out of* the reaction plane. The ratio depends on the transition multipole order, the degree of polarization, and the mixing ratio. Practically, the intensity ratio $R[= I_\gamma(\text{in})/I_\gamma(\text{out})]$ shows greater than unity for stretched quadrupole ($\Delta I = 2$) and unstretched (pure) dipole ($\Delta I = 0$) transitions, while the ratio becomes less than unity for stretched (pure) dipole ($\Delta I = 1$) transitions [10,11]. In the spin and parity assignment, multipolarities of $E1$, $M1$, and $E2$ have been considered since no delayed transition was observed in the present experiment. Information on the γ-ray energies, intensities and *in-* and *out-of-plane* intensity ratios if obtained is summarized in table 1.

Figure 3 shows a level scheme for ^{188}W deduced from the present experimental data. The states up to $I^\pi = 6^+$ in the GSB were known from the previous studies [7,8]. In the present work, we found a 554 keV γ-ray transition in coincidence with the 143, 296, and 432 keV transitions (see fig. 4), extending the GSB up to $I^\pi = 8^+$.

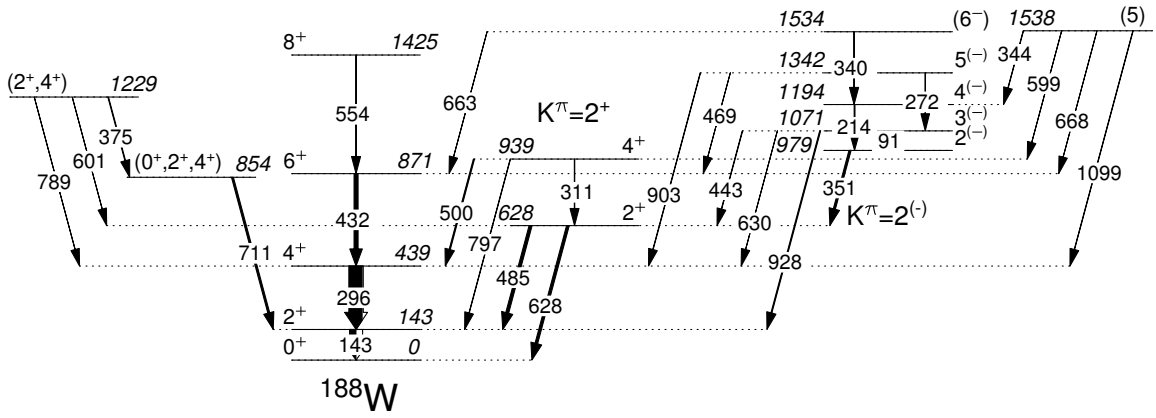

Fig. 3. A proposed level scheme for ^{188}W. The γ-ray and level energies are shown in units of keV. The width of the arrows is proportional to the γ-ray intensities (black) and the calculated intensities of electron conversion (white).

Table 1. Energies E_γ, relative intensities I_γ, and initial level energies E_i for the γ-ray transitions observed in ^{188}W. Intensity ratios I_γ(in)/I_γ(out) for *in-plane* to *out-of-plane* anisotropies are also given.

E_γ (keV)	I_γ	E_i (keV)	I_γ(in)/I_γ(out)
91	< 1	1071	
142.9(1)	53(3)	143	1.13(3)
214.4(1)	5(1)	1194	1.27(18)
271.6(10)	2(1)	1342	
296.3(1)	100(5)	439	1.67(3)
311.3(5)	3(1)	939	
340.0(1)	4(1)	1534	1.03(11)
344.3(4)	2(1)	1538	
351.2(1)	16(2)	979	1.21(8)
375.0(5)	5(1)	1229	
431.6(1)	29(2)	871	1.91(8)
442.5(10)	3(1)	1071	
469.4(10)	2(1)	1342	
484.7(1)	21(3)	628	0.70(3)
499.7(2)	7(1)	939	
554.0(2)	3(1)	1425	2.05(20)
599.3(10)	2(1)	1538	
600.6(10)	2(1)	1229	
628.4(1)	25(7)	628	1.00(5)
630.2(10)	2(1)	1071	
662.5(10)	~ 1	1534	
667.5(10)	~ 1	1538	
711.0(2)	14(3)	854	1.00(4)
788.8(10)	~ 1	1229	
796.5(10)	4(2)	939	1.73(12)
903.0(10)	3(1)	1342	0.81(5)
928.0(5)	7(2)	1071	0.64(3)
1099.0(10)	3(1)	1538	

A 630(2) keV state previously observed is confirmed at 628 keV in the present data, decaying into the 0^+ and 2^+ states in the GSB. In addition, a 939 keV state was newly found above the 628 keV state, connected by a 311 keV transition. These two states likely form a γ vibrational band as explained later. Since the 628 and 939 keV states

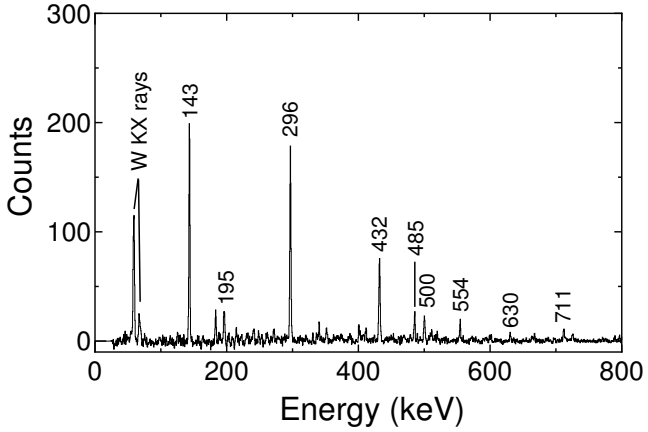

Fig. 4. Sum of coincidence spectra gated on the 143, 296, and 432 keV transitions in ^{188}W.

directly decay to the 0^+, 2^+ and/or 4^+ states in the GSB, the spins and parities of $(1^\pm, 2^+)$ and $(2^+, 3^\pm, 4^+)$ are possible for the 628 and 939 keV states, respectively. However, only the $I^\pi = 2^+$ and 4^+ assignments can be taken for the 628 and 939 keV states according to the following discussion. The value of $R = 1.73(12)$ is consistent with an unstretched dipole or stretched quadrupole assignment for the 797 keV transition, rejecting the $I^\pi = 3^\pm$ assignment for the 939 keV state. In addition, the feeding pattern of the 939 keV state, *i.e.*, the presence of a transition to the GSB 4^+ state and the absence of a transition to the ground state, suggests the $I^\pi = 4^+$ assignment for the 939 keV state rather than the $I^\pi = 2^+$ assignment. This assignment hence excludes the $1^\pm$ assignment for the 628 keV state, and therefore the 628 keV state can be assigned $I^\pi = 2^+$. The value of $R = 0.70(3)$ for the 485 keV transition is consistent with a large negative $E2/M1$ mixing ratio expected [13] for a $\Delta I = 0$ transition from the γ vibrational band to the GSB. The small R value of 1.00(5) for the 628 keV $E2$ transition would be due to de-polarization effects for lower-lying states as seen for the 143 keV $E2$ transition with $R = 1.13(3)$. The intense $\Delta I = 0$ transition to the GSB is a characteristic of γ bands in this mass

region, partly supporting the present spin assignment. Assuming the $\Delta I = 0$ transition to be of $E2$ character, the measured $B(E2)$ ratios of the $\Delta I = 0$ and 2 transitions are 3.1(10) and 18(9) at the $I^\pi = 2^+_\gamma$ and 4^+_γ states, respectively. These are comparable with the values obtained for lighter W isotopes, *e.g.*, 1.9(1) [2.3(1)] at $I^\pi = 2^+_\gamma$ and 5.5(3) [8.6(7)] at $I^\pi = 4^+_\gamma$ in ^{184}W [^{186}W] [14]. Note that the $\Delta I = 0$ transitions from the γ band to the GSB in ^{184,186}W have large negative mixing ratios [14].

A 351 keV transition links a newly observed 979 keV state to the 628 keV state. On top of the 979 keV state, rotational band members which predominantly decay to the GSB were observed. The value of $R = 1.21(8)$ for the 351 keV transition is consistent with an unstretched dipole or stretched quadrupole assignment, leading to the spin and parity assignment of $2^\pm$ or 4^+ for the 979 keV state. However, assuming $\Delta I = 1$ rotational-band sequence, the $I^\pi = 4^+$ assignment can be rejected on the basis of an $I = 3$ assignment for the 1071 keV state. Here, the $I = 3$ assignment is based on the value of $R = 0.64(3)$ for the 928 keV transition. The spin assignments for the 1194 and 1342 keV states were deduced from the anisotropy data for the 214 and 903 keV transitions. The R value for the 340 keV transition is inconclusive for the spin assignment of the 1534 keV state. The $I = (6)$ assignment therefore relies on the $\Delta I = 1$ rotational sequence of this band. The tentative negative-parity assignment for this band was based on the excitation energies of the $K^\pi = 2^-$ octupole states systematically observed at the energies of ~ 1 MeV in the heavy W nuclei [14].

A 1538 keV state was also observed in this experiment. Considering the direct feeding of the $I^\pi = 4^+$ and 6^+ state in the GSB as well as the $I^\pi = 4^{(-)}$ state at 1194 keV, we assign $I^\pi = (5^\pm)$ for the 1538 keV state. Two γ-ray transitions of 195 and 242 keV were observed in coincidence with transitions below the 1538 keV state. Since no detailed connection to lower states was obtained, these transitions are not placed in fig. 3. Two more levels were observed at 854 and 1229 keV. The spin and parity assignments of these levels are inconclusive, and therefore no further discussion will be made in this paper.

4 Discussion

The energy systematics of the GSBs in the even-even W isotopes with $106 \leq N \leq 114$ is shown in fig. 5. The higher energies at each spin state for ^{188}W are consistent with a reduction in deformation for the heavy W isotopes in this region [15]. The energy ratios $R_{4^+/2^+}$ of the $I^\pi = 4^+$ and 2^+ states ($R_{4^+/2^+} = 3.33$ for the rotational limit) are maximized at ^{182}W ($R_{4^+/2^+} = 3.29$) and decrease with neutron number towards ^{188}W ($R_{4^+/2^+} = 3.07$), suggesting less collectivity for the heavy W isotopes. The excitation energies of the γ and octupole vibrational bandheads are also compared in fig. 5, showing the largest values at ^{182}W. Since the excitation energy of the γ vibrational bandhead indicates the softness to γ distortion, the data suggest triaxial softness for the heavy W isotopes. This

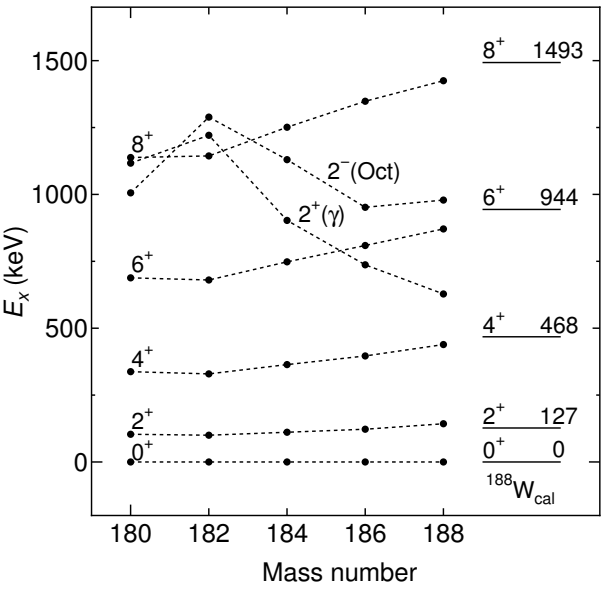

Fig. 5. Energy systematics of the GSBs in the even-even W isotopes with $106 \leq N \leq 114$. The energies for the γ and octupole vibrational bandheads are also plotted. The data except for ^{188}W are taken from ref. [14]. The calculated energies for the GSB in ^{188}W are drawn on the right-hand side.

result is consistent with a shallow minimum against triaxial deformation in potential surface calculations, predicted for the heavy W nuclei, *e.g.*, ^{190}W [2]. The excitation energy of the octupole bandhead slightly increases at ^{188}W as shown in fig. 5. This might indicate that the rigidity against octupole deformation increases at ^{188}W. It is interesting whether this tendency continues in heavier W isotopes, *e.g.*, ^{190}W, or not.

In order to make a microscopic investigation of the GSB in ^{188}W, self-consistent cranking calculations based on the Hartree-Fock-Bogoliubov method [16] have been performed. In the calculation the spherical Nilsson Hamiltonian was chosen for the one-body part in the cranking Hamiltonian, while the so-called $P+Q\cdot Q$ force was chosen for the two-body interaction. The model space consists of two-plus-two major shells for protons and neutrons, and follows the prescription by Kumar and Baranger [17]. Further details of the model are found in ref. [16]. The calculated energies for the GSB in ^{188}W are compared with the observed values in fig. 5. As shown, the calculation reproduces well the observed energy levels. The cranking calculation also predicts slightly positive γ deformation with an almost constant β deformation of ~ 0.19 (see table 2). Similar calculations were performed for the lighter W isotopes with the neutron number of $N = 106$–112 [18]. The observed energy levels of the GSBs are well reproduced within ~ 100 keV. In addition, the calculations predict symmetric prolate shapes for ^{180}W and ^{182}W (*e.g.*, $\gamma < 2^\circ$ at $I = 8\ \hbar$) in contrast to ^{188}W. The triaxial deformation gradually evolves with increasing the neutron number towards ^{188}W. Note that the present γ parameterization follows the Hill-Wheeler definition [19] which has the opposite sign to the Lund convention.

Table 2. Calculated β and γ deformations for the GSB in ^{188}W.

Spin ($\hbar$)	0	2	4	6	8
β	0.190	0.192	0.194	0.196	0.196
γ	0.0°	0.9°	2.8°	4.7°	6.6°

Table 3. Low-lying 2-quasiparticle states in ^{188}W.

K^π	Configuration[(a)]	$E_{\rm mqp}$ (keV)	$E_{\rm res}^{\rm (b)}$ (keV)	$E_{\rm cal}^{\rm (c)}$ (keV)
3^+	$\pi : 1/2^+, 5/2^+$	1871	−150	1721
5^+	$\nu : 1/2^-, 9/2^-$	1768	−150	1618
5^-	$\nu : -1/2^{-(\rm d)}, 11/2^+$	1907	−150	1757
6^+	$\nu : 3/2^-, 9/2^-$	1531	+150	1681
7^-	$\nu : 3/2^-, 11/2^+$	1694	−150	1544
8^+	$\nu : 7/2^-, 9/2^-$	1932	−150	1782
8^-	$\pi : 7/2^+, 9/2^-$	2606	−120	2486
9^-	$\nu : 7/2^-, 11/2^+$	2062	+184	2246
10^-	$\nu : 9/2^-, 11/2^+$	2075	−150	1925

(a) Neutrons (ν): $1/2^-[510]$, $3/2^-[512]$, $7/2^-[503]$, $9/2^-[505]$, $11/2^+[615]$; protons (π): $1/2^+[411]$, $5/2^+[402]$, $7/2^+[404]$, $9/2^-[514]$.
(b) Residual interaction energies are taken from ref. [20].
(c) $E_{\rm mqp} - E_{\rm res}$.
(d) The negative sign corresponds to the unstretched coupling of the spin vectors.

The 1538 keV state is assigned $I = (5)$. The excitation energy and spin are consistent with a 2-quasiparticle excitation. In order to predict low-lying multi-quasiparticle states in ^{188}W, blocked-BCS calculations, of the type described in ref. [20], have been carried out. Deformation parameters $\epsilon_2 = 0.18$ (equivalent to $\beta \approx 0.19$ which is suggested by the self-consistent HFB cranking calculations) and $\epsilon_4 = 0.05$ were used to give the initial set of single-particle states. The single-particle energies for levels close to the Fermi surface used in the calculations were adjusted to reproduce the 1-quasineutron energies in ^{187}W [9] and the 1-quasiproton energies in ^{189}Re [14]. The neutron pairing strength of $G_\nu = 22.3/A$ MeV was chosen so that the calculation reproduces the energy for the known 2-quasineutron $K^\pi = 10^-$ state in the $N = 114$ isotone ^{190}Os, based on the $\nu 9/2^-[505] \otimes 11/2^+[615]$ configuration. On the other hand, the proton pairing strength was chosen to be 1.5 MeV/A higher than the neutron value, *i.e.*, $G_\pi = 23.8/A$ MeV, consistent with ref. [20]. Residual interactions following the Gallagher-Moskowski rules were taken from ref. [20] and included in the calculations. The results for energetically favoured 2-quasiparticle states are shown in table 3. The energy of the 1538 keV state is compared with the energies of the $K^\pi = 5^+$ and 5^- states. Since the blocked-BCS calculations are generally accurate to $\lesssim 160$ keV for 2-quasiparticle states [6], the $K^\pi = 5^+$ assignment is preferred for the 1538 keV state.

In addition to the $K = 5$ states, the blocked-BCS calculations predict several other 2-quasiparticle configurations at low excitation energies as shown in table 3. A low-lying $K^\pi = 7^-$ state is predicted at 1544 keV, which could be isomeric because of its yrast nature. The measurable half-life of isomers in the present work is limited to less than $\sim 5\,\mu$s, on account of the 2 μs TAC range. The $K^\pi = 7^-$ isomer is therefore suggested to have $T_{1/2} \geq 5\,\mu$s, comparable to $T_{1/2} = 18\,\mu$s for the $K^\pi = 7^-$ isomer in ^{186}W [21]. It is also interesting that the calculations predict the yrast $K^\pi = 10^-$ state at 1925 keV, based on the $\nu 9/2^-[505] \otimes 11/2^+[615]$ configuration. Similar isomers with the same configuration are known at 1705 keV in ^{190}Os ($T_{1/2} = 9.9$ m) and 2015 keV in ^{192}Os ($T_{1/2} = 5.9$ s) [14]. Since the present transfer reaction brings in too little angular momentum, an experiment using reactions with heavier-ion beams, *e.g.*, deep inelastic reactions is required for exploring the $K^\pi = 10^-$ state in ^{188}W. It is worth noting that the $K^\pi = 10^-$ state observed in ^{186}W is not isomeric, decaying into a $K^\pi = 9^-$ state with a K-allowed γ-ray transition [21]. This is possibly due to the non-yrast nature of this state. The observed and calculated (without residual interactions) energies of the $K^\pi = 10^-$ state in ^{186}W are 2286 and 2549 keV [22]. The corresponding calculated energy for the $K^\pi = 10^-$ state in ^{188}W is 2075 keV, and the calculated energy including residual interactions is 1925 keV. Since the yrast $I^\pi = 10^+$ state is expected at ~ 2100 keV by extrapolation of the GSB sequence, the $K^\pi = 10^-$ state in ^{188}W is possibly an yrast-trap high-K isomer as observed in ^{190}Os and ^{192}Os.

5 Conclusion

The near-yrast structure of neutron-rich ^{188}W has been investigated using an ^{18}O-induced 2-neutron transfer reaction with a ^{186}W target. In-beam γ-rays were measured in coincidence with scattered ions detected by a high-resolution Si ΔE-E telescope. The ground-state band has been identified up to $I^\pi = 8^+$. The level energies follow the trend of the lighter even-even W isotopes, and are reproduced by self-consistent HFB cranking calculations. In addition, the γ band has been identified. The energy systematics of the γ bandheads is consistent with triaxial softness for the heavy W isotopes. Another $K = 2$ rotational band was observed, and tentatively assigned as the $K^\pi = 2^-$ octupole band on the basis of the energy systematics from lighter W isotopes. A $K = (5)$ state was also observed at 1538 keV. Comparison with blocked-BCS calculations suggests the 2-quasineutron configuration of $1/2^-[510] \otimes 9/2^-[505]$ for this state. The blocked-BCS calculations predict the possible existence of several low-lying 2-quasiparticle states, including $K^\pi = 7^-$ and 10^- states which are suggested to be isomeric because of their yrast nature.

We thank G. Sletten for the preparation of the ^{186}W target and P.D. Stevenson for the discussion on the PES calculations. We also thank the staff of the JAEA tandem accelerator facility for providing the ^{18}O beam.

References

1. R.F. Casten, A.I. Namenson, W.F. Davidson, D.D. Warner, H.G. Borner, Phys. Lett. B **76**, 280 (1978).
2. Zs. Podolyák, P.H. Regan, M. Pfützner, J. Gerl, M. Hellström, M. Caamaño, P. Mayet, Ch. Schlegel, A. Aprahamian, J. Benlliure, A.M. Bruce, P.A. Butler, D. Cortina Gil, D.M. Cullen, J. Döring, T. Enqvist, F. Rejmund, C. Fox, J. Garcés Narro, W. Gelletly, J. Giovinazzo, M. Górska, H. Grawe, R. Grzywacz, A. Kleinböhl, W. Korten, M. Lewitowicz, R. Lucas, H. Mach, M. Mineva, C.D. O'Leary, F.De Oliveira, C.J. Pearson, M. Rejmund, M. Sawicka, H. Schaffner, K. Schmidt, Ch. Theisen, P.M. Walker, D.D. Warner, C. Wheldon, H.J. Wollershiem, S.C. Wooding, F.R. Xu, Phys. Lett. B **491**, 225 (2000).
3. C. Wheldon, J. Garcés Narro, C.J. Pearson, P.H. Regan, Zs. Podolyák, D.D. Warner, P. Fallon, A.O. Macchiavelli, M. Cromaz, Phys. Rev. C **63**, 011304(R) (2000).
4. P.M. Walker, F.R. Xu, Phys. Lett. B **635**, 286 (2006).
5. P.M. Walker, G.D. Dracoulis, Nature (London) **399**, 35 (1999).
6. C. Wheldon, J.J. Valiente-Dobón, P.H. Regan, C.J. Pearson, C.Y. Wu, J.F. Smith, A.O. Macchiavelli, D. Cline, R.S. Chakrawarthy, R. Chapman, M. Cromaz, P. Fallon, S.J. Freeman, A. Görgen, W. Gelletly, A. Hayes, H. Hua, S.D. Langdown, I.Y. Lee, X. Liang, Zs. Podolyák, G. Sletten, R. Teng, D. Ward, D.D. Warner, A.D. Yamamoto, Eur. Phys. J. A **20**, 365 (2004).
7. J.D. Garrett, O. Hansen, Nucl. Phys. A **276**, 93 (1977).
8. Zs. Podolyák, S. Mohammadi, G. De Angelis, Y.H. Zhang, M. Axiotis, D. Bazzacco, P.G. Bizzeti, F. Brandolini, R. Broda, D. Bucurescu, E. Farnea, W. Gelletly, A. Gadea, M. Ionescu-Bujor, A. Iordachescu, Th. Kröll, S.D. Langdown, S. Lunardi, N. Marginean, T. Martinez, N.H. Medina, B. Quintana, P.H. Regan, B. Rubio, C.A. Ur, J.J. Valiente-Dobón, P.M. Walker, Int. J. Mod. Phys. E **13**, 123 (2004).
9. T. Shizuma, T. Hayakawa, S. Mitarai, T. Morikawa, T. Ishii, Phys. Rev. C **71**, 067301 (2005).
10. T. Ishii, S. Shigematsu, M. Asai, A. Makishima, M. Matsuda, J. Kaneko, I. Hossain, S. Ichikawa, T. Kohno, M. Ogawa, Phys. Rev. C **72**, 021301(R) (2005).
11. T. Ishii, S. Shigematsu, H. Makii, M. Asai, K. Tsukada, A. Toyoshima, M. Matsuda, A. Makishima, T. Shizuma, J. Kaneko, I. Hossain, H. Toume, M. Ohara, S. Ichikawa, T. Kohno, M. Ogawa, J. Phys. Soc. Jpn. **75**, 043201 (2006).
12. S. Takeuchi, T. Ishii, M. Matsuda, Y. Zhang, T. Yoshida, Nucl. Instrum. Methods Phys. Res. A **382**, 153 (1996).
13. T. Shizuma, K. Matsuura, Y. Toh, T. Hayakawa, M. Oshima, Y. Hatsukawa, M. Matsuda, K. Furuno, Y. Sasaki, T. Komatsubara, Y.R. Shimizu, Nucl. Phys. A **696**, 337 (2001).
14. ENSDF, NNDC Online Data Service, ENSDF database, `http://www.nndc.bnl.gov/nndc/ensdf/`.
15. R. Bengtsson, S. Frauendorf, F.-R. May, At. Data Nucl. Data Tables **35**, 15 (1986).
16. T. Horibata, N. Onishi, Nucl. Phys. A **596**, 251 (1996).
17. K. Kumar, M. Baranger, Nucl. Phys. A **110**, 529 (1968); M. Baranger, K. Kumar, Nucl. Phys. A **62**, 113 (1965).
18. M. Oi, T. Shizuma, submitted to Phys. Rev. C (2006).
19. D.L. Hill, J.A. Wheeler, Phys. Rev. **89**, 1102 (1953).
20. K. Jain, O. Burglin, G.D. Dracoulis, B. Fabricus, N. Rowley, P.M. Walker, Nucl. Phys. A **591**, 61 (1995).
21. C. Wheldon, R. D'Alarcao, P. Chowdhury, P.M. Walker, E. Seabury, I. Ahmad, M.P. Carpenter, D.M. Cullen, G. Hackman, R.V.F. Janssens, T.L. Khoo, D. Nisius, C.J. Pearson, P. Reiter, Phys. Lett. B **425**, 239 (1998).
22. C. Wheldon, PhD Thesis, University of Surrey (1999), available at `http://www.hmi.de/people/wheldon/`.